

Augumented bioavailability of maltodextrin-based Tenofovir proniosomes via inhibition of MDR1 mediated transport efflux

Swarupa ARVAPALLI ¹ , Anka Rao ARETI ^{2*} 

¹ Department of Pharmaceutics, Research scholar, KL College of Pharmacy, Koneru Lakshmaiah Education Foundation, Vaddeswaram, Andhra Pradesh, 522022, India.

² Department of Pharmaceutics, Associate Professor, KL College of Pharmacy, Koneru Lakshmaiah Education Foundation, Vaddeswaram, Andhra Pradesh, 522022, India.

* Corresponding Author. E-mail: drankarao83@gmail.com Tel. +91-994-846 73 05.

Received: 29 April 2023 / Revised: 12 August 2023 / Accepted: 13 August 2023

ABSTRACT: Tenofovir is an antiviral drug indicated for the treatment of infections caused by the human immunodeficiency virus (HIV) and hepatitis B virus (HBV). TNF is classified as a BCS Class III drug, indicating its ability to readily dissolve in gastrointestinal fluids with poor permeability across intestinal membranes results in a lower absorption rate, ultimately restricting its bioavailability. The primary challenges associated to enhancing the bioavailability of TNF involve intestinal degradation and efflux transport facilitated by Multidrug resistance protein1. TNF-loaded proniosomes were formulated using 3² factorial design by applying slurry method of preparation with a molar ratio of 2.5:1:1.5 for cholesterol, span 60, and maltodextrin, respectively. Maltodextrin-based polymeric nanoparticles exhibited desirable nano-scale properties, including size, polydispersity index, and zeta potentials, which fell within acceptable ranges. The successful PNFs (T-PN3, T-PN4, and T-PN7) demonstrated TNF entrapment in the range of 92.96 to 96.28%. The hydration volume and hydration time of proniosome-based niosomes for delivering TNF were optimized and the results demonstrated the structural homogeneity of niosomes derived from proniosomes. Transmission electron microscopy (TEM) analysis indicated that the niosomes exhibit a uniform and smooth surface morphology. Successful formulations were further characterized for their powder behaviour by angle of repose, TNF interactions with formulation components by FT-IR and DSC thermal analysis. The T-PN3 and T-PN7 formulations demonstrated a high *in-vitro* release rate of approximately 99% in PBS. Additionally, the cellular uptake of TNF from successful PNFs in NCI-N87 cells ranged from 81% to 83%, indicating that T-PN3 and T-PN7 exhibited superior performance compared to free TNF and the commercially available tenofovir. Further mechanistic analysis was conducted using MDR1 efflux studies and western blot techniques. The results demonstrated that both T-PN3 and T-PN7 effectively inhibited the efflux transport of TNF through MDR1 in MDCK-MDR1 and Caco-2 cells.

KEYWORDS: Tenofovir; Proniosomes; Niosomes; MDR-mediated drug efflux; Slurry technique.

1. INTRODUCTION

Tenofovir (TNF), an effective and well-tolerated nucleoside reverse-transcriptase inhibitor (NRTI), exhibits limited absorption leading to reduced oral bioavailability in their available formulations, including oral tablets, oral powder, and oral solutions [1]. This is primarily attributed to a highly charged phosphonate group in its structure, which promotes intestinal degradation and efflux transport mediated by MDR1. Food and Drug Administration (FDA) approved tenofovir disoproxil fumarate (TDF) as a prodrug of tenofovir in 2001, further revolutionizing the management of HIV disease and serving as a critical component of backbone therapy [2]. With the advancement of antiviral therapy, the management of the hepatitis B virus (HBV) has also evolved. The FDA approved TDF for the treatment of HBV in 2008, and it is considered to be one of the most effective treatment options among the eight drugs approved [3, 4]. In 2015, a new formulation of TNF, tenofovir alafenamide (TAF), another prodrug form, received FDA approval [5]. Both TNF prodrugs have demonstrated improved oral bioavailability and pharmacokinetics ranging from 20% to 35% increment due to conversion into their active form, Tenofovir-diphosphate, in various animal and

How to cite this article: Arvapalli S, Areti AR. Augumented bioavailability of maltodextrin-based Tenofovir proniosomes via inhibition of MDR1 mediated transport efflux. J Res Pharm. 2024; 28(5): 1357-1368.

human studies [6-9]. Despite having limited improved bioavailability, TDF and TAF forms appear to be associated with various pharmacokinetic obstacles before reaching systemic circulation, such as stomach acidic pH, exposure to pancreatic & luminal enzymes, higher pHs in the intestinal milieu, and efflux transportation mediated by ABC transporters such as MDR1 [10, 11]. One of the primary challenges concerning TNF's bioavailability is the presence of MDR1-associated drug efflux transport, which restricts transepithelial transport, leading to inadequate absorption and ultimately diminished bioavailability. A recent study showed that MDR1 transporters are actively involved in the efflux transport of TDF across Caco-2 cells [12]. Each obstacle offers a potential opportunity to protect TDF and increase its bioavailability by ensuring stability across a wider pH range, minimizing enzymatic degradation, and blocking MDR1-mediated efflux. Given the multitude of obstacles inherent in the existing formulations of TNF, it is imperative to explore the identification of a novel drug delivery method that can enhance both the bioavailability and stability.

Proniosomes are novel drug delivery systems developed to enhance the bioavailability and stability of drugs with low solubility and/or low permeability. These are dry, free-flowing formulations consisting of a surfactant, a cholesterol source, and the drug of interest that aims to mitigate the limitations commonly associated with liposomes and niosomes. Upon hydration, proniosomes transform niosomes, characterized by a lipid bilayer encapsulating an aqueous core [13]. Proniosomes have demonstrated significant promise in enhancing oral delivery, increasing bioavailability, and facilitating the gastrointestinal absorption of drugs that exhibit limited solubility or permeability [14-17]. By considering the notable attributes of proniosomes compared to other emerging delivery systems, we developed TNF proniosomes to enhance bioavailability by reducing MDR1-mediated transport efflux. This study involved the preparation of TNF proniosomes using a slurry method. Cholesterol, maltodextrin, and span 60 were added to ensure stability of the vesicular membrane, enhance membrane permeability, and act as a non-ionic surfactant agent respectively. To formulations were optimized by 3^2 full factorial design using Design-Expert® software version 8 (Stat-Ease, Inc., Minneapolis, MN, USA). First, proniosomes were physically characterized to understand formulation integrity, followed by the characterization of niosomal dispersions derived from proniosomes. We evaluated various characteristics such as size, PDI, zeta potential, hydration properties, drug entrapment efficiency of the prepared niosomes, and the *in-vitro* release rate of TNF from the optimized formulations. It was determined how the selected formulations accumulate TNF in the gastric environment using NCI-N87 cells.

2. RESULTS

2.1 Entrapment efficiency of Niosomes

The entrapment efficiency of niosomes derived from proniosomes was given in (Table 1).

Table 1. % Entrapment efficiencies of T-PN1 to T-PN16			
PNFs	% EE	PNF's	% EE
T-PN1	62.76 ± 3.11	T-PN9	56.68 ± 3.15
T-PN2	60.24 ± 4.25	T-PN10	65.04 ± 3.67
T-PN3	96.28 ± 3.69	T-PN11	81.28 ± 2.54
T-PN4	93.72 ± 4.85	T-PN12	92.28 ± 3.47
T-PN5	75.08 ± 3.18	T-PN13	73.04 ± 3.58
T-PN6	85.36 ± 3.92	T-PN14	76.72 ± 4.85
T-PN7	92.96 ± 4.15	T-PN15	72.36 ± 5.18
T-PN8	84.08 ± 3.99	T-PN16	89.76 ± 5.49

2.2 Vesicle size, PDI, and Zeta Potential of PNFs

The results for poly dispersibility index, zeta potential, vesicle size was given in (Table 2).

Table 2: Results for PDI, ZP and sizes of PNFs

PNF's	Vesicle size	PDI	ZP
T-PN1	0.698 ± 0.02	0.471 ± 0.03	21.3 ± 1.96
T-PN2	0.751 ± 0.03	0.385 ± 0.02	19.5 ± 1.57
T-PN3	0.947 ± 0.03	0.215 ± 0.01	28.4 ± 2.93
T-PN4	0.931 ± 0.02	0.201 ± 0.01	32.8 ± 3.12
T-PN5	0.642 ± 0.03	0.396 ± 0.02	24.6 ± 2.14
T-PN6	0.769 ± 0.02	0.281 ± 0.02	21.2 ± 1.86
T-PN7	1.034 ± 0.02	0.199 ± 0.01	25.7 ± 2.65
T-PN8	1.123 ± 0.03	0.207 ± 0.02	29.5 ± 2.17
T-PN9	0.783 ± 0.02	0.408 ± 0.03	29.4 ± 2.58
T-PN10	0.724 ± 0.03	0.375 ± 0.02	33.9 ± 2.74
T-PN11	1.056 ± 0.04	0.296 ± 0.01	24.7 ± 1.67
T-PN12	0.987 ± 0.04	0.198 ± 0.01	31.1 ± 2.36
T-PN13	0.786 ± 0.03	0.382 ± 0.02	15.4 ± 1.24
T-PN14	0.654 ± 0.02	0.415 ± 0.03	19.6 ± 1.68
T-PN15	0.891 ± 0.03	0.347 ± 0.02	21.8 ± 1.55

Results represented in Mean ± SD

2.3 Microscopical and TEM analysis

The microscopic TEM images of prepared proniosomes are shown in Figure 1.

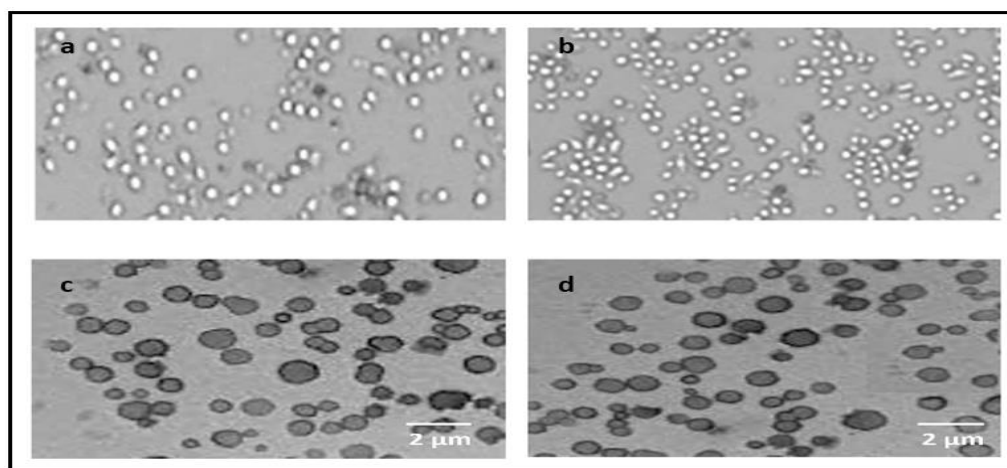


Figure 1. a) Optical photograph of T-PN3 formulation b) Optical photograph of T-PN7 formulation c) TEM image of T-PN3 formulation d) TEM image of T-PN7 formulation.

2.4 DSC Analysis

The DSC curves of different formulations are shown in Figure 2.

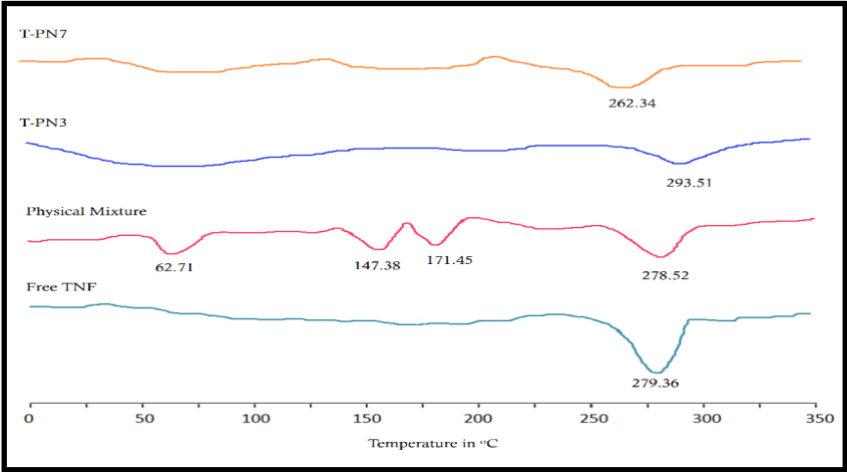


Figure 2. DSC thermograms of (a) pure TNF (b) Physical mixture (c) Maltodextrin containing proniosomal formulations (c) T-PN3 (d) T-PN7.

2.5 *In-vitro* drug release study

The cumulative drug release results are carried out for selected formulations having good zeta potential, vesicle size, entrapment efficiency and the obtained results are given in Table 3.

Table 3: % CDR release from selected TNF- Proniosomes

F.code	% CDR in mins							
	0	15	30	60	120	240	360	480
T-PN3	0	61.24 ± 3.5	76.22 ± 6.2	81.27 ± 5.9	96.27 ± 6.9	97.24 ± 7.1	99.25 ± 6.8	99.36 ± 7.8
T-PN4	0	52.47 ± 4.6	68.29 ± 5.7	75.48 ± 6.8	87.56 ± 7.2	91.85 ± 8.6	94.88 ± 9.3	95.74 ± 8.3
T-PN7	0	59.35 ± 5.1	67.43 ± 5.9	79.81 ± 6.9	93.84 ± 6.3	98.34 ± 7.4	99.24 ± 8.7	99.58 ± 8.6
T-PN8	0	27.36 ± 3.3	41.85 ± 5.3	62.14 ± 7.2	69.18 ± 7.2	71.59 ± 6.2	74.69 ± 8.3	76.95 ± 9.1
T-PN11	0	25.74 ± 2.9	36.85 ± 3.2	49.28 ± 5.2	53.24 ± 6.8	59.38 ± 5.8	62.34 ± 7.3	65.78 ± 7.3
T-PN12	0	19.24 ± 2.1	29.54 ± 2.4	42.57 ± 3.8	49.23 ± 5.1	57.21 ± 6.2	63.59 ± 6.5	69.25 ± 5.9
Free TNF	0	15.24 ± 2.7	23.47 ± 2.1	36.68 ± 2.6	42.15 ± 4.9	46.58 ± 5.7	49.37 ± 5.8	51.69 ± 6.3

2.6 *In-vitro* quantitative cellular uptake of PNFs

The *In-vitro* quantitative cellular uptake of PNFs of selected formulations are shown in Figure 3.

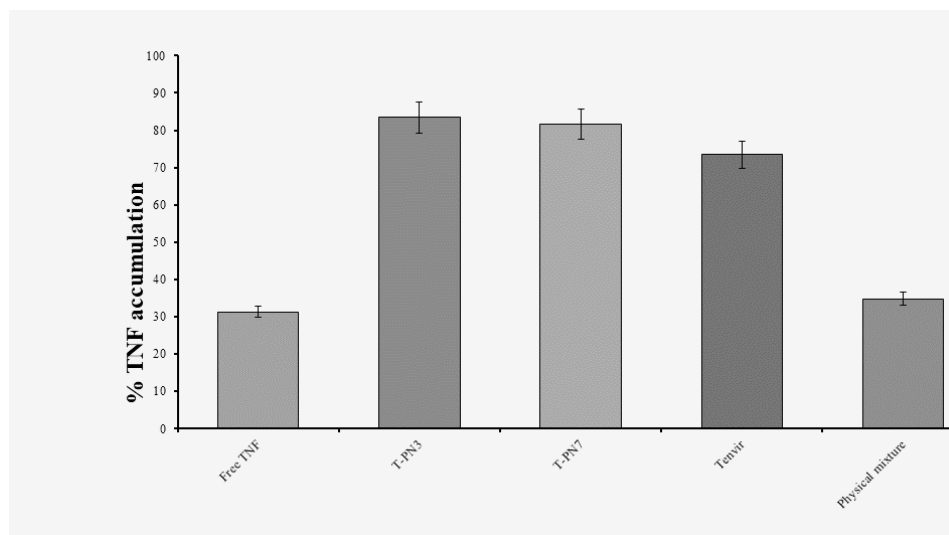


Figure 3. Quantitative cellular uptake of TNF-loaded proniosomal formulations in NCI-N87 cells.

2.7 MDR1 efflux activity

The MDRI efflux activity of selected proniosomes are given in (Table 4, Figure 4).

Table 4. Efflux ratio of different sample types in MDCK-MDR1 and Caco-2 cells.

Sample type	Efflux ratio in MDCK-MDR1 cells		Efflux ratio in Caco-2 cells	
	Without inhibitor	With Inhibitor (colchicine)	Without inhibitor	With Inhibitor (colchicine)
Free TNF	0.74 ± 0.002	0.18 ± 0.003	0.59 ± 0.004	0.11 ± 0.002
T-PN3	0.26 ± 0.001	0.02 ± 0.001	0.17 ± 0.002	0.02 ± 0.001
T-PN7	0.25 ± 0.001	0.02 ± 0.003	0.19 ± 0.005	0.02 ± 0.003
Tenofovir	0.56 ± 0.003	0.05 ± 0.004	0.33 ± 0.003	0.05 ± 0.002

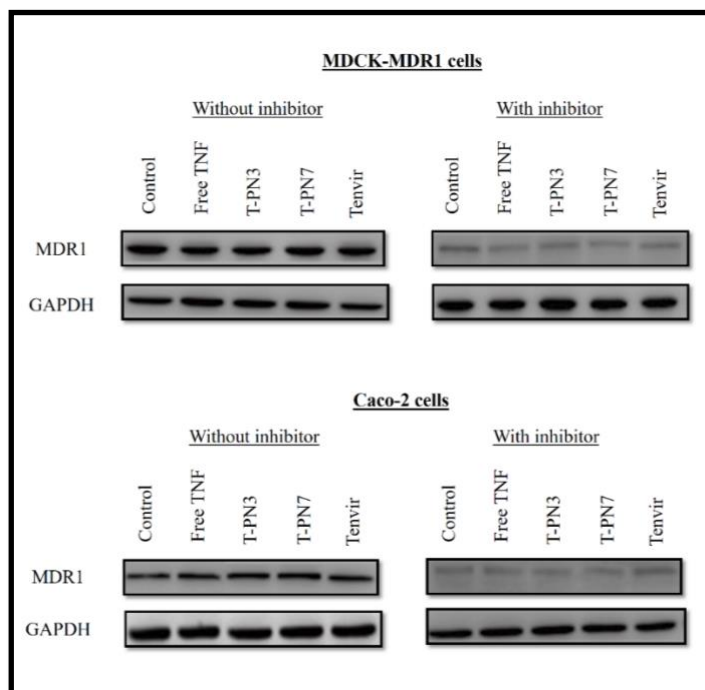


Figure 4. Expression of MDR-1 levels in MDCK-MDR1 and Caco-2 cells after incubating with various PNFs.

3. DISCUSSION

Proniosomes exhibit considerable potential for the encapsulation and delivery of a diverse range of drugs. They have been widely employed for the purpose of drug delivery and targeting, encompassing various administration routes such as oral, parenteral, dermal, transdermal, ophthalmic, vaginal, mucosal, pulmonary, and nasal routes [14]. The utilization of proniosome powders, which are composed of maltodextrin, has been found to enhance the efficacy of oral administration for lipophilic or amphiphilic drugs. This is achieved through their stable carrier properties. The use of maltodextrin as a carrier facilitates enhanced drug loading capacity and provides increased flexibility in adjusting the proportion of surfactant and other constituents. Maltodextrin possesses a notable surface area and exhibits a porous structure, rendering it a suitable medium for the formulation of proniosomes [34]. Several drugs have been effectively formulated via proniosomal formulations. These drugs include vinpocetine, mefenamic acid, lornoxicam, oxybutynin chloride, tolterodine tartrate, risperidone, and estradiol [37-44]. Hence, proniosomal formulations present a versatile drug delivery strategy that exhibits compatibility with a diverse array of pharmaceutical compounds.

The entrapment efficiencies of sixteen proniosomal formulations (T-PN1 to T-PN16) were compared based on a three-level experimental design. The volume of the hydrating medium slightly influenced the % entrapment efficiency. It was found that as the volume of hydrating medium increased from 6 to 15 mL, the % EE decreased. Maltodextrin showed relatively lower PDI values, which denotes the maximum consistency in the niosomal distribution, whereas mannitol investigates the higher PDI score, indicating a diversified niosomal network. The enormous size of the prepared niosomes, which is the primary cause of significant variations in the size distribution as against smaller vesicles, is what causes the heterogeneity of the particle sizes in all niosomal preparations. Larger vesicles, on the other hand, are more likely to entrap drugs. The ZP values for each of the produced niosomes (T-PN1 to T-PN16) were considerable and showed no signs of substantial variation. TEM examination of the niosomes produced from proniosomes revealed spherical vesicles. A discrete and separate collection of vesicles was observed with no evidence of aggregation or agglomeration. It was noted that niosomes had a smooth surface. The DSC data revealed that pure TNF displayed an endothermic abrupt peak at 279.36 °C having a peak value of -31.69 Mw, which represents the melting temperature of TNF. The lack of a distinct peak indicates that the drug's physical state has transformed from crystal to amorphous form, demonstrating its increased solubility and quicker disintegration. An *in-vitro* study of drug release was conducted with the help of drug dissolution apparatus II USP. The release profiles of TNF from PNFs containing capsules are shown in Figure 6. The results

demonstrated that T-PN3, T-PN4, and T-PN7 among all PNFs, showed a burst release of TNF during the first 15 minutes in the range of 52.47 to 61.24 % and then a relatively slow release for about 60 minutes. During the next 60 minutes, a fast release of TNF from these PNFs was observed until 120 minutes, followed by a consistently stable release until the end of the period, about 480 minutes. At the end of 480 minutes, T-PN3 and T-PN7 released the highest release of TNF of 99.36 and 99.58 %, respectively. In contrast, other PNFs, T-PN8, T-PN11, and T-PN12, showed fast release in the range of 42.57 to 62.14 % up to 60 minutes, followed by a relatively stable release until the end of the dissolution period. The maximum cellular absorption of TNF from T-PN3 and T-PN7 was 83.56 % and 81.72 % which is higher than that of tenofovir, showing 73.41% at 4 hours. By contrast, Free TNF and physical mixture showed a similar TNF accumulation of 31.3%, and 34.8% at 4 hours, indicating a poor uptake into NCI-N87 cells. According to these results, proniosomal delivery significantly accelerated the accumulation of TNF from a variety of formulations in the cellular environment. Further, the morphology of NCI-N87 cells was observed and no significant morphological deformation of its original structure was observed following treatment with free TNF, T-PN3, T-PN7, physical mixture, and tenofovir, indicating that there is no affect of PNFs on metabolic and functional activities of the cells even after 24 h of treatment. Proniosomal formulations T-PN3 and T-PN7 achieved maximum transport across MDCK-MDR1 cells from apical to basolateral (A to B) regions at 74.9% and 68.5 %, respectively. As a result of the lower transport of TNF across basolateral to apical regions (B to A), the lower efflux ratios of 0.24 and 0.25 were reported for T-PN3 and T-PN7 respectively. Interestingly, the lowest efflux ratios of 0.17 and 0.19 were observed in intestinal Caco-2 cells for T-PN3 and T-PN7, respectively. Based on these results, proniosomal formulations displayed superior A to B transport when compared with a standard tenofovir formulation in MDCK-MDR1 and Caco-2 cells. The cellular penetration of TNF relies on the architectural composition of the proniosomes. Upon exposure to an aqueous environment, TNF proniosomes undergo hydration, resulting in the spontaneous formation of niosomes. Hydrophilic maltodextrin encapsulate the aqueous core of TNF, while hydrophobic cholesterol organize into a lipid bilayer, thereby providing stability to the niosomal structure. Proniosomes' lipid bilayer fuse with the cell membrane due to their structural similarity. The fusion of proniosomes enables the direct delivery of their contents into the cell cytoplasm, bypassing the endocytic pathway [33]. In addition maltodextrin exhibits mucoadhesive properties, enabling it to adhere to mucous membranes and cell surfaces, facilitating non-specific cellular interactions. Maltodextrin interacts with mucin glycoproteins, the primary constituents of mucus found in mucous membranes. The mucoadhesive properties of maltodextrin are advantageous in drug delivery as they enable extended interaction with target cells and enhance the retention of drug formulations at the administration site [33, 34].

4. CONCLUSION

Based on the analysis and data obtained from the present study, the preparation, optimization, characterization, and potential application of proniosomal formulations (PNFs) as a nanoparticulate tenofovir carrier were well explored. It is recommended that PNF formulated with maltodextrin was proven to be a suitable oral drug delivery vehicle that can be adopted to overcome the current pharmacological limitations of TNF therapy. Further *in-vitro* release and cellular accumulation of TNF in NCI-N87 cells proved the efficacy of maltodextrin-based proniosomal formulations T-PN3 and T-PN7. These two formulations were further proved for the delivery of TNF by blocking the MDR1-mediated efflux transport mechanism in MDCK-MDR1 and Caco-2 cells. The findings of the study could provide a foundation for the creation of more effective oral medication delivery systems as a whole. The results obtained from the Tenofovir proniosomes have been favorable, suggesting future experiments be carried out to examine the suitability of proniosomes with a broader range of drugs that have defined drawbacks for enhanced and effective therapy.

5. MATERIALS AND METHODS

5.1 Materials

Tenofovir was procured from Macleods Pharmaceuticals, Mumbai, India. Cholesterol, Span 60, Maltodextrin and Mannitol were of analytical grade procured from Sigma Aldrich Chemicals, USA, Gibco, BRL (Grand Island, NY), Sisco Research Laboratories (SRL) Pvt. Ltd., Mumbai, India, Merck Chemicals, Mumbai, India.

5.2 Preparation of TNF-loaded PNFs

The slurry technique was chosen to prepare TNF-loaded Proniosomal formulations (PNFs) by utilizing maltodextrin or mannitol as a carrier [9]. Initially, TNF was first digested in an equivalent solution of chloroform and methanol, followed by the required amounts of span 60 and cholesterol Table 5. The contents were mixed thoroughly using a shaker, and with the help of a rotary flash evaporator (Buchirotavapor R-3000, Flawil, Switzerland), the solution was thoroughly dried at 80 rpm under a vacuum (16 mm Hg) at 40 °C until the material in the flask became a powdered and free-flowing substance. They were kept in containers that were firmly covered and kept in a refrigerator (4 °C).

Table 5a. Composition of TNF proniosomal formulations

Components (In mg)	Code of formulation							
	T-PN1	T-PN2	T-PN3	T-PN4	T-PN5	T-PN6	T-PN7	T-PN8
TNF	25	25	25	25	25	25	25	25
Cholesterol	10	10	10	10	15	15	15	15
Span 60	15	30	15	30	15	30	15	30
Maltodextrin	200	200	300	300	200	200	300	300

Table 5b. Composition of TNF proniosomal formulations

Components (In mg)	Code of formulation							
	T-PN9	T-PN10	T-PN11	T-PN12	T-PN13	T-PN14	T-PN15	T-PN16
TNF	25	25	25	25	25	25	25	25
Cholesterol	10	10	10	10	15	15	15	15
Span 60	15	30	15	30	15	30	15	30
Mannitol	200	200	300	300	200	200	300	300

5.3 Experimental design and optimization

A complete 3²-factorial design was devised with the help of Design-Expert® software to assess the impact of different factors on the qualities of TNF-loaded PNF. Three variables were evaluated at two levels (Table 6).

Table 6. 3² factorial design for the optimizing TNF-loaded PNFs.

Table 6.5: Factorial design for the Optimizing PVP-loaded PVPs.		
Factors	Level	
<i>Independent variables</i>		
X ₁ = Quantity of Cholesterol (mg)	10	15
X ₂ = Quantity of Span 60 (mg)	15	30
X ₃ = Quantity of carrier (mg)	200	300
<i>Dependent variables</i>		
Y ₁ = % EE		
Y ₂ = PDI		
Y ₃ = ZP		
Y ₄ = % CDR		

5.4 Characterization of Proniosomes

5.4.1 Determination of TNF %Entrapment efficiency in niosomes

The TNF-loaded niosomes and the unbound TNF were segregated by centrifugation. 1 mL portion niosomal dispersion was centrifuged at 20,000 rpm for one hour at 0 °C. The remnant was mixed with phosphate buffer (pH 6.8) and centrifuged once more after the supernate was discarded. To confirm that the unbound medication was completely evacuated from the crevices between the niosomes, the washing operation was performed twice. To measure the unbound TNF spectrometrically in phosphate buffer at 264 nm, the obtained supernate portions were adjusted to 10 mL by adding phosphate buffer (pH 6.8). This percentage is calculated by deducting the quantity of unbound drug from the total drug infused in 1 mL niosomal dispersion:

$$\%EE = \frac{C_t - C_r}{C_t} \times 100$$

Where C_t and C_r represent concentrations of total TNF and unbound TNF, respectively.

5.4.2. Determination of Vesicle size (PS), Polydispersity index (PDI), and Zeta potential (ZP)

With the use of Zetasizer (NANO-S Malvern Instrument, Worcestershire, UK), the vesicle size was determined for the various niosomal formulations that use the photon dynamic light scattering technique (DLS). Niosomes (0.2 mL) were then dissolved with 1.9 mL of ultrapure water, and then put in an expendable size cuvette for analysis. Samples were subsequently analyzed at 25 °C with a 173 ° scattering angle. In triplicate, the PDI and average particle size were calculated. A foldable capillary cell was utilized for zeta potential determination, measurements were taken using the same concentration of niosomal dispersion, and measuring the zeta potential of the samples [10].

5.4.3. Microscopical and Transition Electron Microscope (TEM) analysis

By using optical microscope with a magnification of 1000x, the niosomal dispersion was observed for vesicle structure. JEOL transmission electron microscopy (TEM; Model: JEM-2100F, Tokyo, Japan) was used to analyze specific TNF-loaded niosomal dispersions.

5.4.4. Differential Scanning Calorimetry (DSC)

DSC study was carried out for pure tenofovir and selected PNFs to detect fluctuations in their melting points. A definite quantity of 6-10 mg of samples (tenofovir and optimized TNF-loaded PNFs) were analyzed with the help of a DSC-60 differential scanning calorimeter [13]. The apparatus entailed the calorimeter (DSC 60), thermal analyzer (TAWS 60), flow controller (FCL 60), and operating software (TA 60). Briefly, the samples were positioned in aluminium crucibles, and a blank crucible was employed for reference, with nitrogen constantly flowing at 20 mL/min. During the analysis, a temperature between 50-330 °C was used at a heating rate of 10 °C/min, and nitrogen was utilized as a gasification agent.

5.4.5. In-vitro release studies

TNF-loaded PNFs' solubility was contrasted against that of pure TNF. The USP type II dissolution equipment was used for the dissolution investigations (paddle method). A hard gelatin capsule containing samples (TNF-loaded PNFs and pure TNF) amounting to 25 mg of TNF was used. The experiment was carried out using a dissolving media that contained 730 mL of 0.1N HCl (pH 1.2), 270 mL of 0.2 M tribasic sodium phosphate (pH 6.8), followed by 7 more hours of testing. The temperature was held at 37±1°C while mixing at a speed of 100 rpm. Samples (5ml) were taken out at different times (15, 30, 60, 120, 240, 360, and 480 min), followed by filtering with a 0.45 µm filter membrane, and then assessed at 264 nm. The dissolution tests were carried out three times.

5.4.6. *In vitro* cellular uptake of TNF-PNFs

To proceed, NCI-N87 gastric cells were planted in 6-well plates (2×10^5 each) in order to quantitatively determine the cytoplasmic drug concentration. The Dulbecco's Modified Eagle's Medium (DMEM) was changed out for new medium following the incubation time, and Free TNF, T-PN3, T-PN7, and physical mixture were introduced to get a desired concentration of TNF equal to $10 \mu\text{M}$. This was followed by a 4-hour incubation period at 37°C . After incubating, the medium was removed, and the cells underwent two PBS washes to get rid of the free proniosomal form. Following a recovery centrifugation at 1000 rpm, the recovered cells were suspended in PBS with 1x triton-100 solution. Subsequently, an ultrasonic lyser was used to lyse the cells for five minutes in a water bath. Then the cell lysate was centrifuged to remove cell debris at 15,000 g and the supernate was withdrawn. The amount of TNF in the collected supernate was quantified with the help of High performance liquid chromatography (HPLC).

5.5. MDR1 efflux activity

In achieving bioavailability, multidrug resistance, or resistance to chemically unrelated drugs entering the cytoplasm, poses the greatest challenge. In 12-well CostarTranswell plates (Corning Inc.), MDCK-MDR1 and Caco-2 cells were implanted (3×10^5 cells each) onto polycarbonate membranes. Cells were incubated for 3 days, forming confluent monolayers. With the help of a Millicell-ERS device from Millipore, the integrity of the monolayer was evaluated by measuring the transepithelial electrical resistance (TEER) across the monolayer. The adsorbing permeability and sensitivity for MDR1-mediated efflux were assessed in independent studies through the addition of free TNF, and proniosomal formulations T-PN3, T-PN7, and tenofovir at a concentration of $10 \mu\text{M}$ equivalent to TNF, with or without $5 \mu\text{M}$ colchicine (MDR1 inhibitor). The apical chamber was filled with all of the test samples. An analysis of propranolol (non-substrate) and colchicine (substrate) demonstrated the MDR efflux transporter's efficiency. Three replications of cell monolayers were maintained at 37°C for two hours while being shaken (at 160 rpm). After being incubated, samples were taken from the basolateral and apical chambers, and their test substance levels were measured using HPLC. Values for mass transfer A to B, and B to A, for various formulations, with or without inhibitor were calculated using quantitative estimation [11, 12].

Acknowledgements: I would like to acknowledge K.L College of Pharmacy for providing facilities to carry out this research.

Author contributions: Concept – S.A.; Design – S.A., A.A.; Supervision – A.A; Resources – S.A; Materials – S.A; Data Collection and/or Processing – S.A.; Analysis and/or Interpretation – S.A.,A.A.; Literature Search –S.A.; Writing – S.A.; Critical Reviews –A.A.

Conflict of interest statement: “The authors declared no conflict of interest”

REFERENCES

- [1] Wassner C, Bradley N, Lee Y. A review and clinical understanding of tenofovir: Tenofovir disoproxil fumarate versus tenofovir alafenamide. J Int Assoc Provid AIDS Care. 2020; 19:2325958220919231. <https://doi.org/10.1177/2325958220919231>
- [2] U.S. Food and Drug Administration Approves Gilead's Biktarvy® (Bictegravir, Emtricitabine, Tenofovir Alafenamide) for Treatment of HIV-1 Infection. <https://www.gilead.com/news-and-press/press-room/press-releases/2018/2/us-food-and-drug-administration-approves-gileads-biktarvy-bictegravir-emtricitabine-tenofovir-alafenamide-for-treatment-of-hiv1-infection>. (accessed on february 07,2018).
- [3] Hepatitis B (who.int). <https://www.who.int/publications/i/item/9789241549059> (accessed on march 01,2015).
- [4] Terrault NA, Lok ASF, McMahon BJ, Chang KM, Hwang JP, Jonas MM, Brown RS Jr, Bzowej NH, Wong JB. Update on prevention, diagnosis, and treatment of chronic hepatitis B: AASLD 2018 hepatitis B guidance. Hepatology. 2018; 67(4):1560-1599.
- [5] De Clercq, E. Tenofovir alafenamide (TAF) as the successor of tenofovir disoproxil fumarate (TDF). Biochem Pharmacol. 2016;119:1-7. <https://doi.org/10.1016/j.bcp.2016.04.015>
- [6] Kearney B, Flaherty J, Shah J. Tenofovir disoproxil fumarate clinical pharmacology and pharmacokinetics. Clin Pharmacokinet. 2004;43(9):595–612. <https://doi.org/10.2165/00003088-200443090-00003>
- [7] Naesens L, Bischofberger N, Augustijns P, Annaert P, Mooter G, Arimilli M, Kim C, Clercq E. Antiretroviral efficacy and pharmacokinetics of oral bis(isopropylloxycarbonyloxymethyl)-9-(2-

- phosphonylmethoxypropyl)adenine in mice. *Antimicrob Agents Chemother.* 1998;42(7):1568–1573. <https://doi.org/10.1128%2Faac.42.7.1568>
- [8] Shaw JP, Sueoka CM, Oliyai R, Lee W, Arimilli M, Kim C, Cundy K. Metabolism and pharmacokinetics of novel oral prodrugs of 9-[(R)-2-(phosphonomethoxy)propyl]adenine (PMPA) in dogs. *Pharm Res.* 1997;14(12):1824–1829. <https://doi.org/10.1023/a:1012108719462>
- [9] Barditch-Crovo P., Deeks S.G., Collier A, Safrin S, Coakley D, Miller M, Kearney B, Coleman R, Lamy PD, Kahn J, McGowan I, Lietman PS. Phase I/II trial of the pharmacokinetics, safety, and antiretroviral activity of tenofovir disoproxil fumarate in human immunodeficiency virus-infected adults. *Antimicrob Agents Chemother.* 2001;45(10):2733–2739. <https://doi.org/10.1128/aac.45.10.2733-2739.2001>
- [10] Celum C, Baeten JM. Tenofovir-based pre-exposure prophylaxis for HIV prevention: evolving evidence. *Curr Opin Infect Dis.* 2012; 25(1):51-57. <https://doi.org/10.1097%2FQCO.0b013e32834ef5ef>
- [11] Zhang L, Strong JM, Qiu W, Lesko LJ, Huang SM. Scientific perspectives on drug transporters and their role in drug Interactions. *Mol Pharm.* 2006;3(1):62-69. <https://doi.org/10.1021/mp050095h>
- [12] Gelder J, Deferme S, Naesens L, De Clercq E, van den Mooter G, Kinget R, Augustijns P. Intestinal absorption enhancement of the ester prodrug tenofovir disoproxil fumarate through modulation of the biochemical barrier by defined ester mixtures. *Drug Metab Dispos.* 2002; 30(8):924-930. <https://doi.org/10.1124/dmd.30.8.924>
- [13] Radha GV, Rani TS, Sarvani B. A review on proniosomal drug delivery system for targeted drug action. *J Basic Clin Pharm.* 2013;4(2):42-48.
- [14] Song S, Tian B, Chen F, Zhang W, Pan Y, Zhang Q, Yang X, Pan W. Potentials of proniosomes for improving the oral bioavailability of poorly water-soluble drugs. *Drug Dev Ind Pharm.* 2015;41:51–62. <https://doi.org/10.3109/03639045.2013.845841>
- [15] Aburahma MH, Abdelbary GA. Novel diphenyl dimethyl bicarboxylate provesicular powders with enhanced hepatocurative activity: preparation, optimization, in vitro/in vivo evaluation. *Int J Pharm.* 2012;422:139–150. <https://doi.org/10.1016/j.ijpharm.2011.10.043>
- [16] Veerareddy PR, Bobbala SKR. Enhanced oral bioavailability of isradipine via proniosomal systems. *Drug Dev Ind Pharm.* 2013; 39:909–917. <https://doi.org/10.3109/03639045.2012.717945>
- [17] Sahoo RK, Biswas N, Guha A, Kuotsu K. Maltodextrin based proniosomes of nateglinide: Bioavailability assessment. *Int J Biol Macromol.* 2014;69: 430–434. <https://doi.org/10.1016/j.ijbiomac.2014.05.075>
- [18] Bhavsar DS, Patel BN, Patel CN. RP-HPLC method for simultaneous estimation of tenofovir disoproxil fumarate, lamivudine, and efavirenz in combined tablet dosage form. *Pharm Methods.* 2012; 3(2):73-78. <https://doi.org/10.4103/2229-4708.103876>
- [19] Chandra A, Sharma PK. Proniosome-based drug delivery system of piroxicam. *Afr J Pharm Pharmacol.* 2008; 2(9): 184–190.
- [20] Lohumi A. A novel drug delivery system: Niosomes review. *J Drug Deliv Ther.* 2012; 2. <https://doi.org/10.22270/jddt.v2i5.274>
- [21] Okore VC, Attama AA, Ofokansi KC, Esimone CO, Onuigbo EB. Formulation and evaluation of niosomes. *Indian J Pharm Sci.* 2011; 73: 323–328.
- [22] Gurrapu A, Jukanti R, Bobbala SR, Kanuganti S, Jeevana JB. Improved oral delivery of valsartan from maltodextrin based proniosome powders. *Adv Powder Technol.* 2012; 23: 583–590. <https://doi.org/10.1016/j.apt.2011.06.005>
- [23] Wen MM, Farid RM, Kassem AA. Nano-proniosomes enhancing the transdermal delivery of mefenamic acid. *J Liposome Res.* 2014; 24: 280–289. <https://doi.org/10.3109/08982104.2014.911313>
- [24] Thiel-Demby VE, Tippin TK, Humphreys JE, Serabjit-Singh CJ, Polli JW. In vitro absorption and secretory quotients: practical criteria derived from a study of 331 compounds to assess for the impact of P-glycoprotein-mediated efflux on drug candidates. *J Pharm Sci.* 2004;93(10):2567-2572. <https://doi.org/10.1002/jps.20166>
- [25] Troutman MD, Thakker DR. Novel experimental parameters to quantify the modulation of absorptive and secretory transport of compounds by P-glycoprotein in cell culture models of intestinal epithelium. *Pharm Res.* 2003;20(8): 1210-1224. <https://doi.org/10.1023/a:1025001131513>
- [26] Batrakova EV, Li S, Vinogradov SV, Alakhov VY, Miller DW, Kabanov AV. Mechanism of pluronic effect on P-glycoprotein efflux system in blood-brain barrier: contributions of energy depletion and membrane fluidization. *J Pharmacol Exp Ther.* 2001; 299(2):483-493.
- [27] Gilbaldi M, Perrier D. *Pharmacokinetics*. 2nd ed. New York: Marcel Dekker; 1982. p. 409–417.
- [28] Mokhtar M, Sammour OA, Hammad MA, Megrab NA. Effect of some formulation parameters on flurbiprofen encapsulation and release rates of niosomes prepared from proniosomes. *Int J Pharm.* 2008; 361: 104–111. <https://doi.org/10.1016/j.ijpharm.2008.05.031>
- [29] Debnath A, Kumar A. Structural and functional significance of niosome and proniosome in drug delivery system. *Int J Pharm Eng.* 2015; 3: 621–637.
- [30] Kakar R, Rao R, Goswami A, Nanda S, Saroha K. Proniosomes: An emerging vesicular system in drug delivery and cosmetics. *Pharm Lett.* 2010; 2: 227–239.
- [31] Nasr M. In vitro and in vivo evaluation of proniosomes containing celecoxib for oral administration. *AAPS PharmSciTech* 2010; 11: 85–89. <https://doi.org/10.1208%2Fs12249-009-9364-5>

- [32] Atnip A, Giusti MM, Sigurdson GT, Failla ML, Chitchumroonchokchai C, Bomser JA. The NCI-N87 cell line as a gastric epithelial model to study cellular uptake, trans-epithelial transport, and gastric anti-inflammatory properties of anthocyanins. *Nutr Cancer*. 2020;72(4):686-695. <https://doi.org/10.1080/01635581.2019.1644354>
- [33] Yasam VR, Jakki SL, Natarajan J, Kuppusamy G. A review on novel vesicular drug delivery: Proniosomes. *Drug Deliv*. 2014; 21, 243-249. <https://doi.org/10.3109/10717544.2013.841783>
- [34] Sengodan T, Sunil B. Formulation and evaluation of maltodextrin-based proniosomes loaded with indomethacin. *Int J Pharm Tech. Research*. 2009; 3:517-523.
- [35] Zhang L, Strong JM, Qiu W, Lesko LJ, Huang SM. Scientific perspectives on drug transporters and their role in drug Interactions. *Mol Pharm*. 2006;3(1):62-69. <https://doi.org/10.1021/mp050095h>
- [36] Srivalli K, Lakshmi PK. Overview of P-glycoprotein inhibitors: a rational outlook. *Braz J Pharm Sci*. 2012;48(3):353-367. <https://doi.org/10.1590/S1984-82502012000300002>
- [37] El-Laithy HM, Shoukry O, Mahran LG. Novel sugar esters proniosomes for transdermal delivery of vinpocetine: preclinical and clinical studies. *Eur J Pharm Biopharm*. 2011; 77:43-55. <https://doi.org/10.1016/j.ejpb.2010.10.011>
- [38] Wen MM, Farid RM, Kassem AA. Nano-proniosomes enhancing the transdermal delivery of mefenamic acid. *J Liposome Res*. 2014; 24:280-289. <https://doi.org/10.3109/08982104.2014.911313>
- [39] Madan JR, Ghuge NP, Dua K. Formulation and evaluation of proniosomes containing lornoxicam. *Drug Deliv Translat Res*. 2016; 6:511-518. <https://doi.org/10.1007/s13346-016-0296-9>
- [40] Soliman SM, Abdelmalak NS, El-Gazayerly ON, Abdelaziz N. Novel non-ionic surfactant proniosomes for transdermal delivery of lacidipine: optimization using 23 factorial design and in vivo evaluation in rabbits. *Drug Deliv*. 2016; 23:1608-1622. <https://doi.org/10.3109/10717544.2015.1132797>
- [41] Rajabalaya R, Leen G, Chellian J, Chakravarthi S, David SR. Tolterodine tartrate proniosomal gel transdermal delivery for overactive bladder. *Pharmaceutics*. 2016; 8:27. <https://doi.org/10.3390%2Fpharmaceutics8030027>
- [42] Imam SS, Aqil M, Akhtar M, Sultana Y, Ali A. Formulation by design-based proniosome for accentuated transdermal delivery of risperidone: in vitro characterization and in vivo pharmacokinetic study. *Drug Deliv*. 2016;22:1059-1070. <https://doi.org/10.3109/10717544.2013.870260>
- [43] Fang JY, Yu SY, Wu PC, Huang YB, Tsai YH. In vitro skin permeation of estradiol from various proniosome formulations. *Int J Pharm*. 2001; 215:91-99. [https://doi.org/10.1016/s0378-5173\(00\)00669-4](https://doi.org/10.1016/s0378-5173(00)00669-4)
- [44] Ammar H, Ghorab M, EL-Nahhas S, Higazy I. Proniosomes as a carrier system for transdermal delivery of tenoxicam. *Int J Pharm*. 2011;405:142-152. <https://doi.org/10.1016/j.ijpharm.2010.11.003>
- [45] Illamola SM, Valade E, Hirt D, Dulioust E, Zheng Y, Wolf JP, Tréluyer JM. Development and validation of an LC-MS/MS method for the quantification of tenofovir and emtricitabine in seminal plasma. *J Chromatogr B Analyt Technol Biomed Life Sci*. 2016;1033-1034: 234-241. <https://doi.org/10.1016/j.jchromb.2016.08.011>